Cell Reports
Physical Science

CellPress
OPEN ACCESS

Article

Continuous humidity pump and atmospheric water harvesting inspired by a tree-pumping system

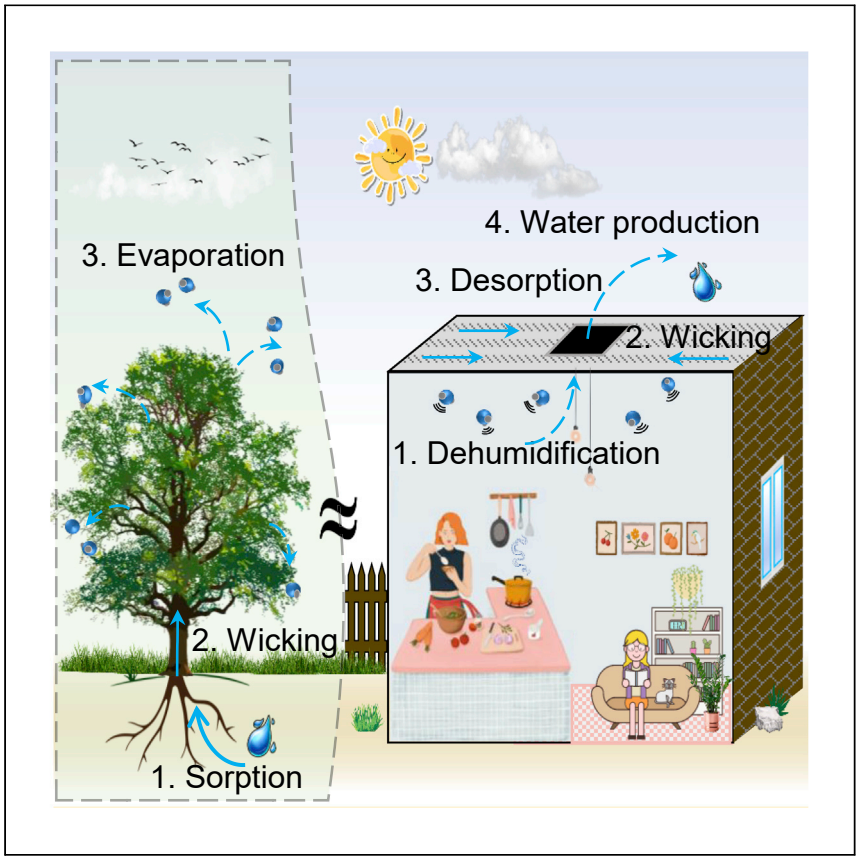

Entezari et al. develop an efficient sorbent-based simultaneous dehumidification and atmospheric water-harvesting strategy that involves the design of devices that combine sorption, capillary effect, and radiative cooling. This approach exhibits excellent humidity regulation and water production performance across a wide range of humidity in residential buildings.

Akram Entezari, He Lin, Oladapo Christopher Esan, Weili Luo, Ruzhu Wang, Ruoyu You, Liang An

rzwang@sjtu.edu.cn (R.W.)
ruoyu.you@polyu.edu.hk (R.Y.)
liang.an@polyu.edu.hk (L.A.)

Highlights

Wicking can replace moving parts of dehumidifiers and shorten regeneration cycles

The strategy can be applied in buildings for dehumidification and water harvesting

It is possible to produce 40.6 $g/d/m_{air}^3$ of water while maintaining the RH between 50% and 70%

Entezari et al., Cell Reports Physical Science 4, 101278
February 15, 2023
https://doi.org/10.1016/j.xcrp.2023.101278

Cell Reports
Physical Science

CellPress
OPEN ACCESS

Article

Continuous humidity pump and atmospheric water harvesting inspired by a tree-pumping system

Akram Entezari,[1] He Lin,[1,2] Oladapo Christopher Esan,[1] Weili Luo,[3] Ruzhu Wang,[3,*] Ruoyu You,[4,*] and Liang An[1,5,*]

SUMMARY

Dehumidification not only regulates the relative humidity (RH) of buildings with reduced cooling costs but also provides a potential drinking water source for residents. Desiccant-based dehumidification has a lower energy consumption than the condensation-based method; however, the former requires successive regeneration of used sorbents and is, therefore, bulky. In this study, by mimicking transpiration in trees, we propose a humidity pump (HP) that continuously dehumidifies rooms by creating a continuous driving force for water wicking. Meanwhile, we investigate the potential of the HP by combining it with atmospheric water harvesting systems. We use activated carbon-lithium chloride composites since they have proven to possess high sorption capacity and strong capillary effect. We develop a small prototype, and our results show that it can maintain the RH between 50% and 70% while producing 1.3–3.25 g water per day. By advancing these techniques, we create an opportunity for developing more energy-efficient humidity regulation and atmospheric water harvesting systems.

INTRODUCTION

As dehumidification plays a pivotal role in the energy consumption of buildings, interest in ambient humidity regulation has grown in recent years. Building heating, ventilation, and air conditioning systems account for approximately 40% of their total energy consumption, and relative humidity (RH) is a key energy determinant.[1,2] By dehumidification, the RH decreases and not only facilitates reaching and maintaining the preset temperature but also makes higher temperatures more tolerable (due to a lower heat index). Less cooling is thus necessary, and energy can be saved. In addition, dehumidification harvests indoor atmospheric moisture, which is a freshwater resource, showing an interesting potential for sustainable water management in residential buildings.

Dehumidification is the process of removing moisture from the air to decrease the vapor pressure (humidity ratio) from the initial value to the target value. It normally uses two methods: cooling-based and desiccant-based dehumidification (see Figure 1). Cooling-based dehumidification involves cooling the air entering a room to its dew point and extracting water from the air in liquid form. In addition, since the air is cooler than the acceptable range, it is reheated before entering the room (see the blue line in Figure S1A). Thus, a lot of energy is consumed in cooling the air to its dew point and then reheating the dried air back to a comfortable temperature. Recently, studies have shown that cold surfaces provided by infrared radiating (IR) cooling selective emitters can passively condense water in RHs higher than

[1]Department of Mechanical Engineering, The Hong Kong Polytechnic University, Hung Hom, Kowloon, Hong Kong SAR, China

[2]Institute of Textiles and Clothing, The Hong Kong Polytechnic University, Hung Hom, Kowloon, Hong Kong SAR, China

[3]Institute of Refrigeration and Cryogenics, Shanghai Jiao Tong University, 800 Dongchuan Road, Shanghai 200240, China

[4]Department of Building Environment and Energy Engineering, The Hong Kong Polytechnic University, Hung Hom, Kowloon, Hong Kong SAR, China

[5]Lead contact

*Correspondence: rzwang@sjtu.edu.cn (R.W.), ruoyu.you@polyu.edu.hk (R.Y.), liang.an@polyu.edu.hk (L.A.)

https://doi.org/10.1016/j.xcrp.2023.101278

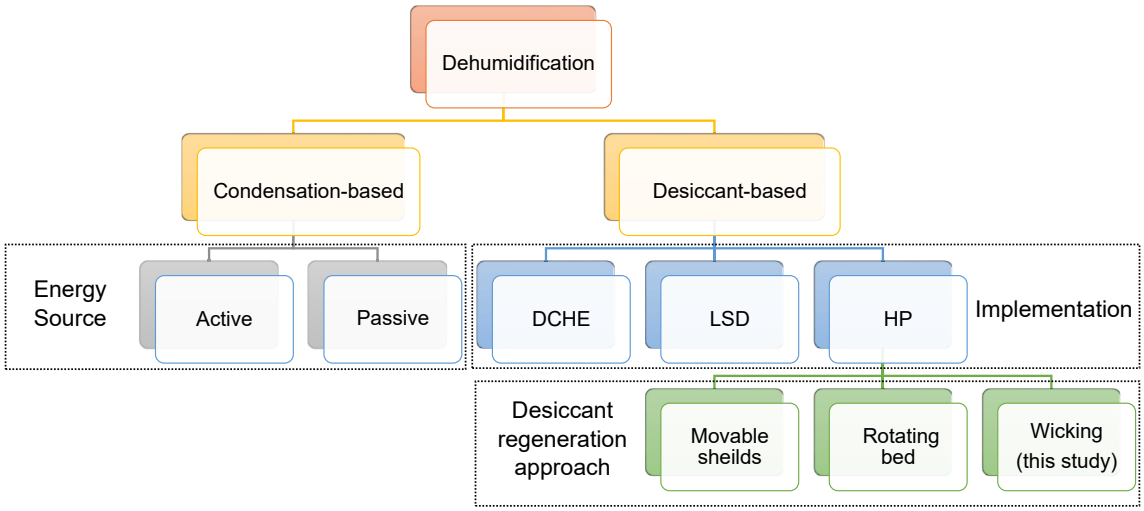

Figure 1. Classification of dehumidification methods in the building sector
DCHE, desiccant coated heat exchanger; LDS, liquid sorbent dehumidification.

65% to counteract this disadvantage[3]; however, they are in their early stage and have a low power density.

Dehumidification by desiccants involves the absorption of indoor moisture by hygroscopic materials. Traditional desiccant-based dehumidification systems perform by placing a large bed containing sorbent in room,[4,5] which is not only bulky, but can also cause a temperature increase indoors because of the exothermic sorption reaction. Other methods involve placing desiccants entering the room, where air circulates, which heats the air because of the released sorption heat, requiring a post-cooling process (see the orange line in Figure S1A). In addition, periodically heating the desiccant material is necessary to regenerate it for continuous use. Recent years have seen more attention given to this method and several concepts have been proposed to overcome the issues in the traditional systems, such as desiccant-coated heat exchanger[6,7] (see Figure S1B), liquid sorbent dehumidification[8–10] (see Figure S1C), and humidity pump (HP).

A humidity pump (HP)[11–13] is the newest concept based on a desiccant-modified method that can be implemented in the walls or roof of a building and can sorb humidity from an interior environment and transfer it to the outside. In this concept, the sorbent is first exposed to the indoor air, and the interior RH gradually drops. As time passes; the sorbent captures more water and its moisture-absorbing capability decreases. To regenerate this sorbent, two methods have been previously proposed.

1. In the first method of regenerating sorbent in the HP, a frame for sorbent is designed, which has two movable shields at both sides of the sorbent. One shield separates the sorbent from the outside during the dehumidification process, while the other shield is open, and the sorbent is exposed to the indoor humid air. When the sorbent reaches the point that it needs to be regenerated, the inner shield closes to disconnect the sorbent from the indoor humid air, while the outer shield opens to expose the sorbent to a heat source such as sun lights to desorb the sorbed water. To achieve continuous dehumidification, two panels of sorbent can be installed in a room. Cao et al.[12] developed two multilayer HP panels using silica gel, MIL-101(Cr), carbon black, and a

phenolic foam that allows the penetration of moisture from indoor (adsorption) to outdoor (desorption). A prototype with two shields was designed and established (see Figure S1D), successfully dehumidifying indoor RH from 65% to 58% in 2 h. This HP system does not show very high desorption performance and suffers from a complicated sorbent synthesis process, expensive material, moving parts, and a short time regeneration period (approximately 10 min).

2. In the second method of regenerating sorbent in the HP, the sorbent is coated on both sides of a rotating surface. While the sorbent on one side is exposed to indoor air and is extracting humidity from the air, the other side (which is exposed to the outdoor environment) experiences regeneration by heating. When the sorbent facing indoors becomes saturated, the HP system rotates and the function of sorption-desorption on the two surfaces is changed. Both cooling and heating functions on a surface are possible by using thermoelectric modules (TEs) and changing the applied electric field direction. Li et al.[11] coated 82 g of silica gel on two heat sinks and installed them on both sides of a TE module and placed the whole structure on the ceiling of a cabinet (size: 80 × 50 × 80 cm) (Figure S1E). By integrating the system into a wall, it was possible to decrease the humidity from 98% to 60% in 1 h. As can be seen in the green line in Figure S1A, this system avoids overheating (as in desiccant-based dehumidification) or overcooling (as in condensation-based dehumidification). However, it must be noted that TE is not energy efficient, and this HP system suffers from high energy consumption, as it requires moving parts with short cycle times (10 min). All of these disadvantages lead to a 1.5 °C increase in the indoor temperature in only 1 h of operation.

It is worth mentioning that there is a new study that reported a concept for a one-step (simultaneous sorption-desorption) indoor dehumidification.[13] A 6 cm × 6 cm developed material (with PAN, MIL-101[Cr], LiCl and carbon black) was installed on the roof of a room as an HP, and it decreased the indoor RH from 70% to 60% in 2 h under one sun illumination (Figure S1F). However, the performance needs to be faster, and they used metal-organic frameworks (MOFs), which is not cost effective on large scales.

Additionally, all previous HP studies are carried out in a sealed box without any humidity generation inside. This insolated interior is quite different from the real world. Daily routine activities of human beings, such as cooking, planting, and bathing, release humidity. Furthermore, even vital life functions, such as respiration and perspiration, release water, which is referred to as "insensible water loss," must be accounted for when calculating dehumidification performance. A 70-kg man, for example, sweats 400 mL per 24 h due to respiration and 400 mL due to perspiration. Even this amount of water from human vital activities would increase the humidity of a room the size of (4 m × 4 m × 5 m) from a dry RH of 40% to 100% (see Note S1 and Tables S1 and S2). Therefore, to ascertain the actual performance of any dehumidification system, including HP, it is necessary to include a humidity generator within the experiment box. Thus, previously reported HP systems generally have several disadvantages, including complicated sorbent development procedures, expensive materials, moving parts, energy-intensive regeneration process, and low energy efficiency, as well a lack of a humidity generator inside the box.

Learning from transpiration in trees, where water is absorbed in the roots and then pumped up to the leaves against gravity and evaporating in the leaves (Figure 2A), herein, we propose a compact and easy-to-scale HP-atmospheric water harvesting

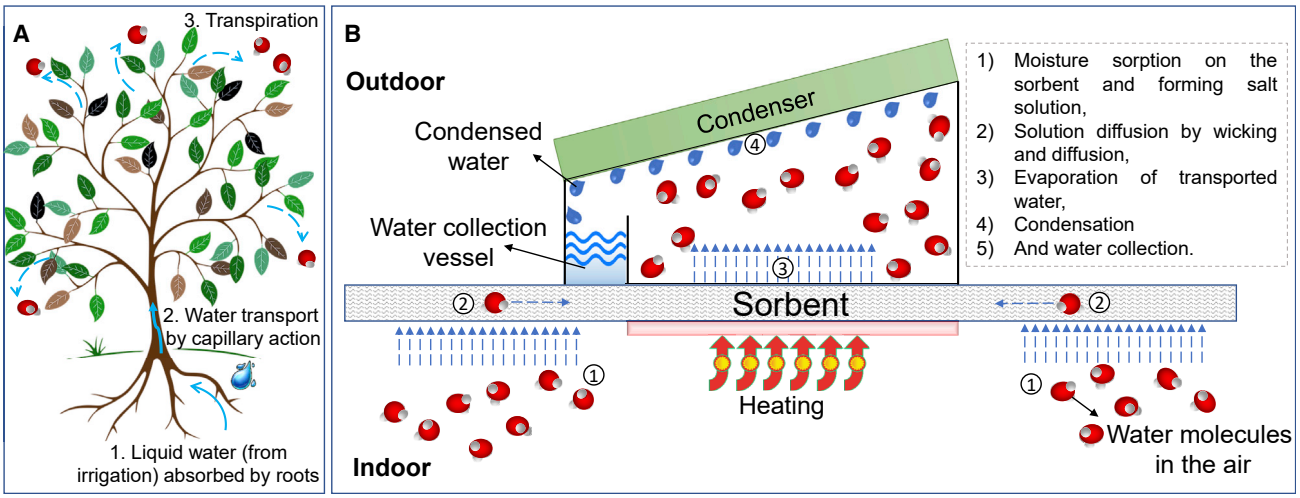

Figure 2. Mechanism of water pumping in plants and our proposed mimic of tree-inspired design for HP-AWH

(A) Plants use a capillary pump system to obtain water: roots absorb water and leaves transpire, which in turn causes tree trunks to draw water up from the ground level.

(B) Analogy between the water pump in trees and our proposed HP-AWH. The roles of sorption sites, desiccant body, and desorption sites moisture in HP-AWH correspond with the core elements in a tree with the same numbers. The insert on the right side represents the mechanism. A continuous transmission of water molecules outdoors from indoors occurs through sorption on a sorbent surface that is exposed indoors (in the way roots do so), wicking through the desiccant layer (in the way trucks do so), and evaporation in the middle portion of sorbent confined inside the desorption chamber (in the way leaves do so). The liquid water path is shown in solid lines while the vapor path is displayed in dashed lines.

(AWH) for humidity control and water production. This concept combines a passive refrigerate-free cooling device and solid desiccant materials with a capillary effect, which replaces the moving parts of HP with a passive water-wicking force. A proof-of-concept device is fabricated by using an activated carbon fiber-based (ACF) sorbent, an IR emitter, and a commercial heater. ACF-LiCl composites were used since they have good sorption and wicking properties.[14–18] The inexpensive developed ACF-LiCl desiccant layer exhibits an unprecedented moisture sorption capacity of 2–3 kg m^{-2}, an acceptable wicking performance, as well as superior long-term stability, enabling dehumidification in conjunction with AWH. Additionally, the IR emitter is developed as the condenser, which displays a 7 °C cooling effect, thus promoting water condensation.

This HP-AWH concept exhibits 2.69 kWh kg^{-1} dehumidification energy consumption and an average dehumidification rate of 19.94 g m^{-2} h^{-1} under vigorous water input each cycle of extracting water from indoor air collects approximately 9.75 g of water per cubic meter of dehumidified air. To the best of our knowledge, there have not been any previous studies on HP-AWH systems. Continuous indoor dehumidification in the presence of a humidity generator with periodic water production by using IR-emitter cooling is an entirely new concept. This work reveals that an ACF-based desiccant and IR emitter can potentially be applied for simultaneous dehumidification (HP) and efficient AWH.

RESULTS

Operating principle and device design

In trees, roots passively transport water to leaves via the xylem. The capillary effect forms a column of water molecules in the xylem, and the water is transported through wicking to the mesophyll, where it evaporates from the leaves surface and escapes from the plant through the stomata. With this unique functional

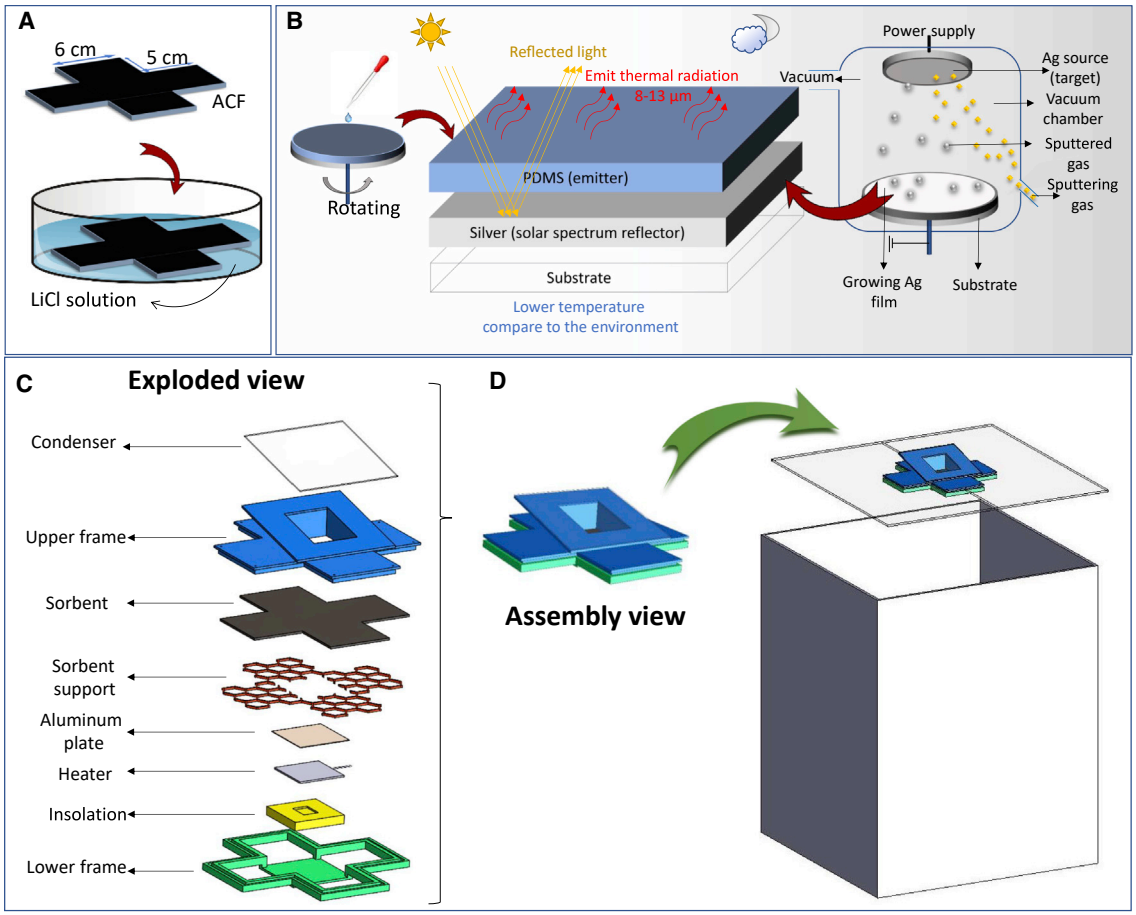

Figure 3. Preparation and assembly of the proposed HP-AWH components

(A) Schematic illustration of wicking sorbent fabrication.

(B) Structure of a multilayer emitter condenser (middle) prepared using plasma-enhanced physical vapor deposition of Ag as a solar spectrum reflector (right insert) and PDMS as a thermal radiative emitter in the sky window range (left insert).

(C) Diagram of the prototype.

(D) Assembly diagram of the proposed concept using ACF-LiCl and the IR-emitter cooler.

characteristic in mind, a design of HP-AWH was developed where sorbents with a high wicking potential can be considered as a substitute for moving parts, and sorbed water can be transferred from sorption sites to the desorption chamber. As shown in Figure 2B, moisture is sorbed on the open parts of the sorbent and forms a salt solution (①), the formed solution is passively transferred to the covered parts of the sorbent by wicking and diffusion (②), transported water evaporates by localized heating (③), and condenses under a multilayer IR emitter (④), allowing condensed water to be collected in the designed vessel (⑤).

ACF has been used to demonstrate wicking performance in previous studies, which can transport aqueous solution by capillary effect.[14,19] Therefore, ACF-LiCl composites can be considered as a suitable sorbent for the HP-AWH concept, where LiCl is responsible for sorbing moisture from indoor air, and the sorbed water molecules can be transferred to the desorption part via the capillary effect of ACF hairs. Figure 3A shows sorbent preparation by impregnation method. Also, multilayer IR-emitters have been developed as a condenser by using plasma-enhanced physical Ag vapor deposition and a polydimethylsiloxane (PDMS) spin coating (Figure 3B;

for more information, see Note S2 and Figure S4) following the study by Haechler et al.[3] Here, PDMS was chosen as a thermal emitter since it is inexpensive, chemically stable, and easily prepared, as well as being suitable for near-black infrared emitters for cooling applications.[3,20,21]

As illustrated in Figure 3C, we developed a proof-of-concept prototype, which mainly includes a "+" shape sorbent, two sorbent holder frames, an insulator, a 4 W electric heater (4 cm × 4 cm), an aluminum sheet (5 cm × 5 cm), four plastic mesh supports, and the developed IR emitter (as a condenser). This shape was chosen for the sorbent to minimize dead zones in the sorbent (see Note S3 and Figure S5). As can be seen in the picture, the sorbent was placed between two frames where its four wings sorb indoor moisture and transfer it to the middle part (desorption part), which sits on an electric heater that separates it from the interior. To install this prototype on the roof of the testing box, some challenges need to be overcome.

One critical challenge of implementing our device was to avoid dropping off the sorbent after sorbing water and getting heavy. Thus, a plastic mesh with large holes was devised under each wing to keep the sorbent in place. Another key challenge in our design was to provide adequate and safe heat transfer between the desiccant material and the heater while minimizing heat transfer into the interior environment. To solve this, the top side of the heater was attached to an aluminum sheet, and insulation material was filled in the gap between the heater's lower surface and indoors. Also, since the tests were conducted in a controlled environment inside the building, using an IR emitter was impossible. Therefore, we evaluated the developed emitter's performance in outdoor conditions. The results indicate that the temperature of the emitter is approximately 7°C lower than the ambient temperature (see Note S4 and Figure S6). Thus, we provide this cooling effect using a thermoelectric (bought from TE cooler, HT009075) in our following test. For more detail and photos see Note S5 and Figures S7–S9.

To check the performance of the developed HP-AWH prototype, a scaled-down model of a house was constructed with dimensions of 40 cm × 40 cm × 50 cm, and a roof window with the shown shape in Figure 3D was designed for prototype installation. The box was kept in a multifunctional room with a constant temperature and humidity. First, we checked the sorbent sorption, desorption, and wicking performance. Second, we investigated the dehumidification performance of sorbents, without any humidity generator inside the box. Third, we checked the performance of the humidity generator without any sorbent inside the prototype. Last, we dissected the proposed HP-AWH prototype in the presence of a humidity generator, where (1) the sorbent reduces the RH of the box below 70% (HP function), by dehumidifying the box from its initial high RH and continuously absorbing water input from the humidity generator, and (2) the cyclic sorbent regeneration (from the center, which is not exposed to the indoor environment and gets wet indirectly by wicking in sorbed water at its wings), and then condensing and collecting the desorbed water (AWH function).

Experimental characterization of the sorbent

The sorbent fabrication began with immersing ACF in different concentrations of LiCl solution (0%, 20%, and 30% LiCl solution), and then the water sorption capacity of these three samples was evaluated at 23 °C. The isotherm curves were generated using modified ASAP 2020.[22] The results are presented in Figure 4A. As can be seen, the composites containing salt can sorb more water compared with pure ACF, and the composite with a higher salt content have a greater sorption capacity.

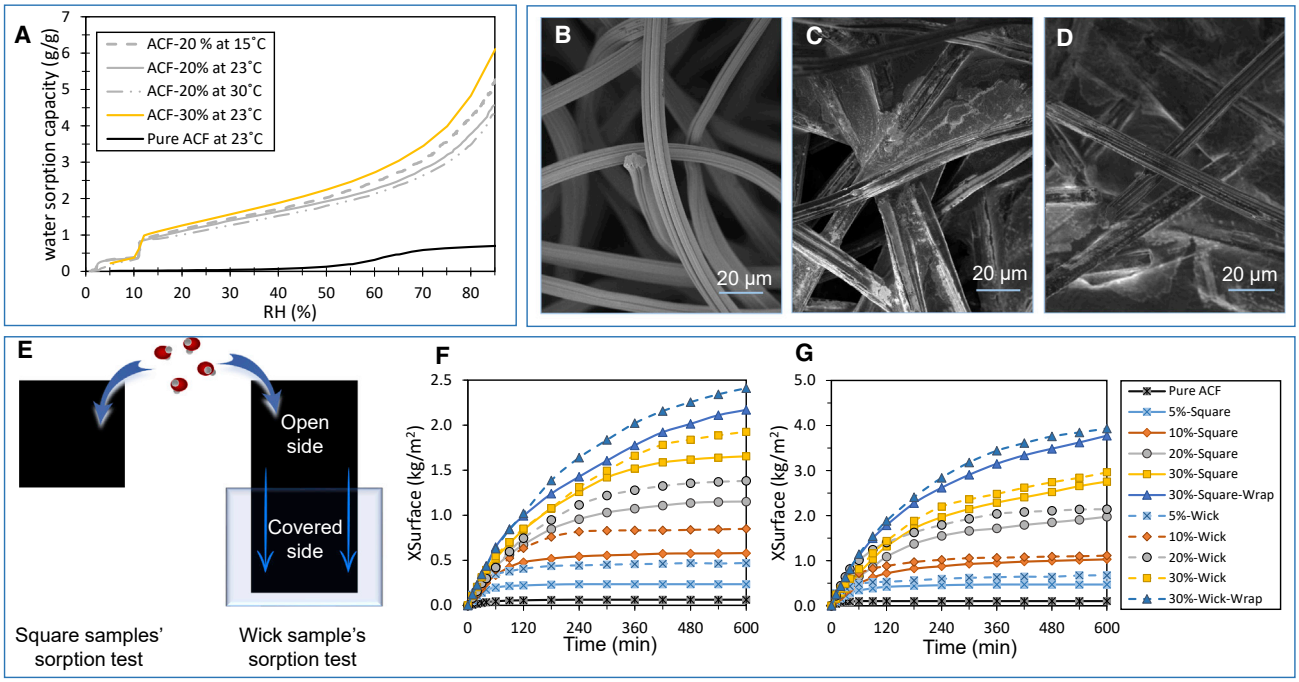

Figure 4. ACF-LiCl composite made of different salt solution concentrations and their water sorption isotherms, SEM and sorption, and sorption-wicking kinetics

(A) Water sorption isotherms of pure ACF and its composites with 20% and 30% LiCl solutions.

(B–D) Morphology of ACF (B), ACF-20% (C). and ACF-30% (D). Scale bar, 20 μm.

(E) A schematic illustration of the sorption mechanism on a square and a wick sample.

(F and G) The amount of absorbed water on one square meter of sorbent in 40% of RH (F) and 70% of RH (G).

Furthermore, to evaluate isotherms in different temperatures, composite with 20% LiCl is fabricated and tested at 15 °C and 30 °C. As can be seen in Figure 4A, the sorption capacity of samples slightly decreases with increasing temperature, which shows that the sorption capacity is a weak function of temperature in the normal ambient temperature range.

The samples topology was evaluated by a scanning electron microscope (SEM) image to demonstrate the samples' wicking properties (more SEM pictures are shown in Figure S2, and pores' information and salt percentages of each composite are presented in Tables S3 and S4). As can be seen in Figures 4B and 4C, ACF composites still keep the parent ACF structure, and they will be able to store sorbed water because of their small hairs acting as small capillaries.

To further evaluate the sorption kinetics and wicking performance of composites and salt content effect on them, square-shaped samples (5 cm × 5 cm) and wick samples (5 cm × 10 cm) were prepared with different salt solutions (0%, 5%, 10%, 20%, and 30% LiCl solution). The wick samples were made with a rectangular shape and the same width as the square-shaped samples (5 cm), but their length is twice their width (10 cm). In these samples, only one-half of the sorbent is in direct contact with the air. A schematic illustration of sorption on a square and a wicked sample is shown in Figure 4E and real pictures are shown in Figure S10. The samples were evaluated at 30 °C and two levels of RHs, namely, a RH of 40% as representative of dry condition and RH of 70% as high humidity.[15,18,22–24] Since the square sample made with 30% salt solution showed leaking, two more samples of these composites were made and

covered with a cotton fabric, which are described as "wrapped" samples. The prepared samples were placed in a constant humidity and temperature chamber with preset conditions and their kinetics and capacity were evaluated.

The volumetric sorption capacity is very important in AWH systems[25]; however, immersion of ACF sheets in the salt solution affects composites' thickness and makes calculating accurate volume hard. Therefore, we reported sorption capacity based on surface which can be easily measured by simple tools (gravimetrically evaluation is also available in Note S6 and Figure S11). **Xsurface** is defined as the amount of sorbed water per 1 square meter of sorbent surface (kg m^{-2}).[26] As observed in Figure 4F after 10 h, the moisture sorption capacities of pure ACF, 5%-Square, 10%-Square, 20%-Square, 30%-Square, and 30%-Square-Wrap at 40% RH reached 0.06, 0.24, 0.58, 1.15, 1.66, and 2.17 kg m^{-2}, respectively. Furthermore, to observe water harvesting behavior in high RHs, we placed square samples in a RH of 70%. The results are depicted in Figure 4G. The moisture sorption capacities of pure ACF, 5%-Square, 10%-Square, 20%-Square, 30%-Square, and 30%-Square-Wrap at 70% RH reached 0.10, 0.47, 1.03, 1.97, 2.76, and 3.77 kg m^{-2}, respectively.

As can be seen in Figures 4F and 4G, it is evident that the moisture sorption capacity of wick samples is not twice that of the square samples, except in 5% samples, even though the sorbent mass was doubled. However, the benefit of wick samples is shown in conditions with high RH, where the 30%-Square sample starts leaking while the wick samples can store extra water in their covered tails and prevent leaking into the prototype (having a salt solution leak into the experiment box is generally not acceptable).

To investigate the amount of water sorbed by the covered tail, we selected the best two wick samples (namely, 20%-Wick, and 30%-Wick). The wrap sample was not chosen because its performance, in conjunction with desorption, was not superior to that of the non-wrapped sorbents (see Note S7). The selected samples were placed in the chamber with an RH of 40% and 70% and a temperature of 30 °*C* for 24 h. To achieve desired conditions, a constant temperature and humidity chamber was used (Table S8 describes the characteristics of the chamber). As mentioned, in the wick samples only one-half of the sorbent is directly exposed to the humid air. The samples were cut in half at the end of testing, and the part exposed to humid air was determined to be the open side, while the other half was determined to be the covered side. The weight of each part was recorded, and then each was transferred to the oven to be dried at 80 °C. Samples were weighed after they were dried. Results are summarized in Table S5. We can see that the covered side includes almost 52%–56% of the wet sample weight. Likewise, the percentage of sorbed water indicates that the covered side is storing more water at a RH of 70%; however, at a RH of 40%, water is almost equally distributed in the open and covered sides. The dry weight of each part shows that the uniform salt distribution got disordered and the covered side is heavier. This could be expected from wet samples, where the 20%-Wick and 30%-Wick samples still had unsolved crystals after 24 h in covered sides (Figure S3). However, we see a better degree of uniformity in the salt content of 20% composite compared to corresponding values in the 30%-Wick sample. Thus, 20%-Composites can fully meet the needs of practical applications HP-AWH.

An additional test was conducted to determine the simultaneous sorption, wicking, and desorption behaviors in a single component. Two sorbent composites in the shape of "+" were prepared by immersing ACF in 20% and 30%, and they were labeled PS-20% and 30%-PS, respectively. The center of the dry samples with a

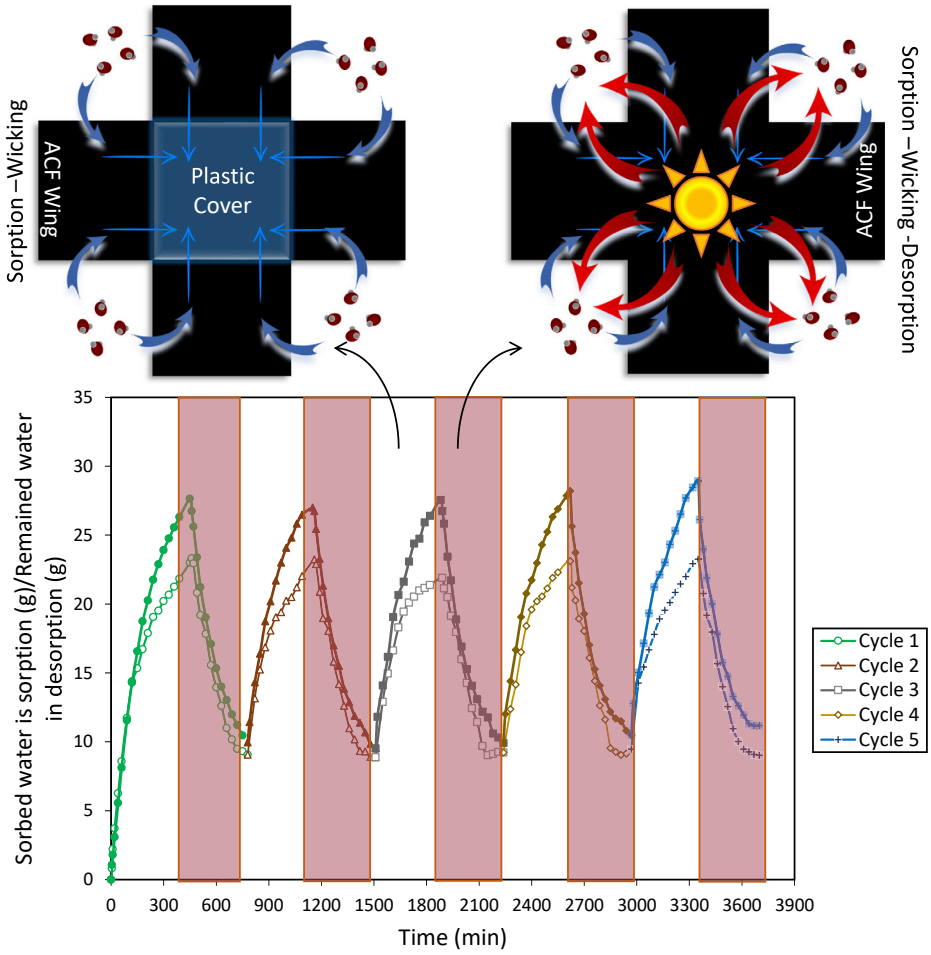

Figure 5. Cyclic sorption-wicking process in the chamber followed by sorption-wicking-desorption process under one sun solar simulator irradiation

PS-20% is shown in hollow markers, and 30%-SP are shown in filled markers. The dry samples were placed in the chamber with pre-defined temperature and RH to complete sorption-wicking process and their absorbed water mass (g) was reported; then the samples were conveyed and placed under solar illumination to for sorption-wicking-desorption process and the remained water in the samples was recorded. These two processes were repeated five times for each sample. The sorption-wicking-desorption half-cycles are highlighted in light red in this figure.

size of 6 cm × 6 cm was covered by a plastic bag and placed in a chamber with preset conditions of 30 °C and 70% RH. Then, 7.5 h later, the samples were taken out, the plastic bags were removed, and the samples' center was immediately placed under a solar simulator with a diameter of 6 cm for 5.5 h. Desorption performance under one sun solar irradiation intensity was chosen based on these experiments (Note S8 and comparison of Figure S12A vs. Figure S12B).

We used a solar simulator because it was impossible to heat only the middle part of the samples by heating them in the oven. Also, a circular irradiation pattern was used due to the limitations of the solar simulator, which prevented us from using square-shaped irradiation. A shield was also installed around the solar simulator projector to prevent unwanted sunlight from radiating the sample's wings. The weight of the samples was recorded over time and depicted in Figure 5. The environmental conditions were controlled by using a chamber that had a RH of 60%–70% and a temperature of 23 °C–25 °C. We repeated these experiments for five cycles to ensure that the sample can periodically sorb and desorb water. For the new cycles, there was a 6-h sorption period and a 6-h desorption period.

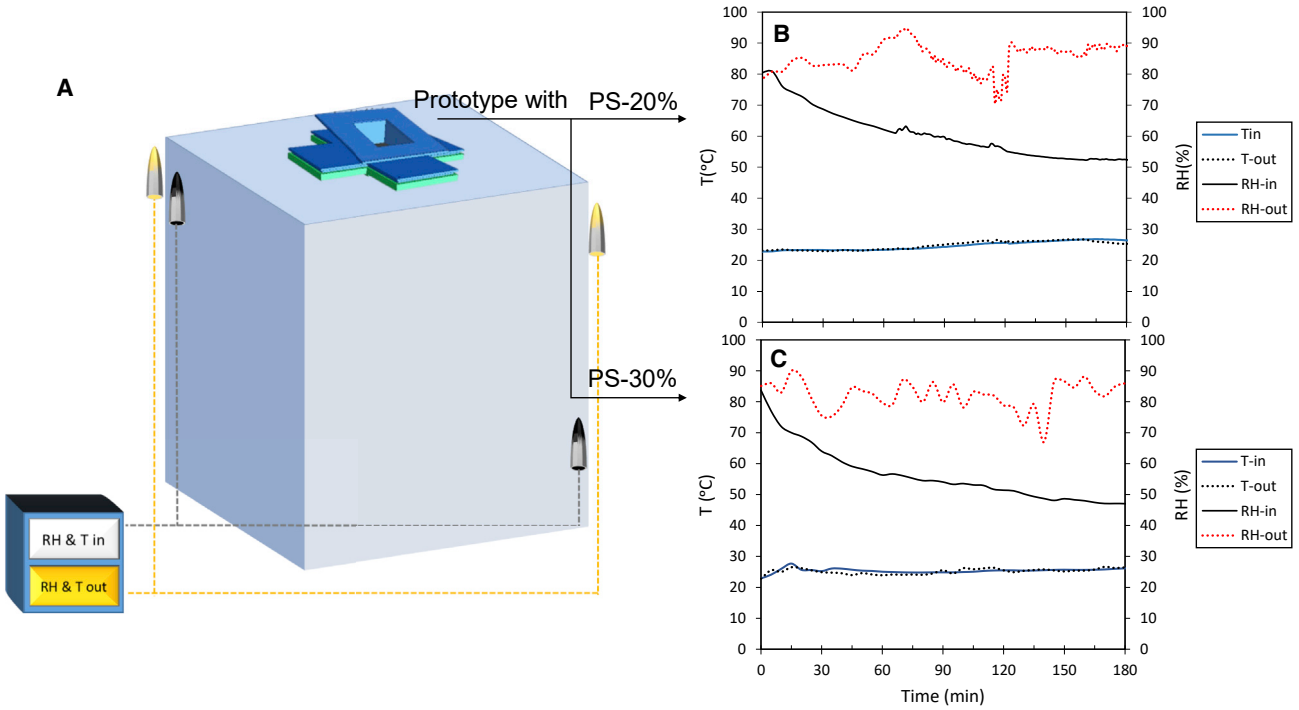

Figure 6. Dehumidifying performance of selected samples in a box with a humidity generator

(A) A Schematic figure of the testing setup.

(B) Indoor and outdoor T and RH of the box when PS-20% is implemented in the prototype.

(C) Indoor and outdoor T and RH of the box when PS-30% is implemented in the prototype. The sensors are placed inside and outside the box with 10 cm distance from bottom and roof of the box. The test took place from January 20 to 21, 2022.

It is important to wisely choose the desorption period and crystallization of salt in the middle part during desorption must be avoided, otherwise, the sorption performance will reduce since these salt crystals will be trapped in the middle part which is not directly in contact with humid air during sorption process. To determine the behavior of the sorbent in a long-term sorption-wicking-desorption test, we extend the desorption time to one day. Figure S13 and Video S1 show the sample has flexible wings, but the center is completely dried. This proves that sorption and desorption can be accomplished in two different sorbent sites and with the aid of wicking.

Box with the sorbent but without humidity generation

In light of the results of the sorption-desorption tests on the square and wicking samples, two ACF composites made of 20% and 30% salt solutions were chosen for inclusion in the prototype. They were constructed with a shape that could be fitted inside the prototype (PS-20% and PS-30%) and were tested for their ability to dehumidify a house model box. The humidity of the environment was set to high RH (>70%). The temperature and RH of the box inside were continuously recorded and shown in Figure 6. After 3 h of using PS-30%, the box RH decreased from 85% to 47.0%, whereas using PS-20% reduced the box RH from 80% to 52.4%.

The results seem to place the dehumidification capacity on par with previous studies.[11–13] In previous HP studies, the initial RH of the testing box was lower than the RH of the environment. It should be noted that our study (as well as the previous studies) used greater quantities of sorbent, so regeneration was not required.[4,11] We still cannot refer to it as a disadvantage of our prototype because,

in our experiment and previous studies, the amount of water vapor inside the boxes was quite small. By removing only 0.553 g of water from saturated air in a box with dimensions 40 cm × 40 cm × 50 cm, the RH of the air will decrease from 100% to 60% at 25 °C. Only 2 g of the weakest sorbents, such as mesopores silica gel, can adsorb this amount of water at this condition.[27,28] This means that dehumidification in a sealed box is not very impressive or difficult; however, all studies of HPs measure the effectiveness of their device in sealed boxes.

It would, therefore, make more sense to consider a source of humidity in the box of the HP test. The following two sections investigate the dehumidification performance of our prototype in the box with a humidity generator inside, which is more practical for real-world applications of humidity control in a room space with residents.

Box with humidity generation but without sorbent inside

Two methods could be used to simulate the humidity generation function in the experiments and create more realistic testing conditions. In the first method, known quantities of liquid water can be injected at predetermined times. However, there is no guarantee that all the injected water will evaporate. The second approach involves placing a solution containing water inside the box and measuring the amount of water evaporated over time. In response to the RH of the box, the second method will dictate the amount of evaporated water (as in real conditions, where the water evaporation rate from surfaces and bodies is higher in the lower RHs). Therefore, we chose the second method.

To start, we conducted intensive tests to investigate the effect of humidity generation type and size in the box. (For more information, please refer to Table S9 and Figure S14, as well as Table S10 and Figure S15.) Note S9 presents the results in detail. It was discovered that a 50-mL water container with a 4.8-cm diameter can represent real conditions. It is worth mentioning that, by using a larger beaker, for instance with a 9.2-cm diameter, the RH of the box can be increased to 85%, which is favorable for the AWH function in our concept. Meanwhile using this size, the condition is equivalent to the presence of five to seven people in a small 4 m × 4 m room, and to achieve the expected HP performance with such a high humidity generation rate, the prototype needs more regeneration cycles, which requires more labor work and goes beyond the time frame of academic work.

After selecting the right solution and size for the humidity generator, the testing box was initially dehumidified to less than 40% using a desiccant. After that, a 50-mL beaker (D = 4.8 cm) containing 73 g water was substituted for the desiccator, and the box was sealed. Figure 7 shows the mass of the evaporated water, RH, and the temperature inside (RH-in and T-in) and outside (RH-out and T-out) of the box. The outside temperature was 23 °C–25 °C, and the average RH was 70%. The lack of air movement inside the box causes the temperature inside to be slightly higher than the outside temperature. During the first 24 h, the RH inside increased rapidly from 39.35% to 69.55%, and then gradually increased to 74.15% the following day. Thereafter, the RH level remained constant. In general, the rate of water evaporation remains at a constant value of 1.64 g/d. Because the prototype is 1,000 times smaller than a real room and the average person produces 700 mL of water vapor per day, placing this beaker inside the box is equivalent to the presence of 2.3 people in a 4 m × 4 m × 5 m room.

According to the mass balance of water in the box, once we reach steady-state mode, no evaporation of water is expected in a sealed box. Here it is evident that

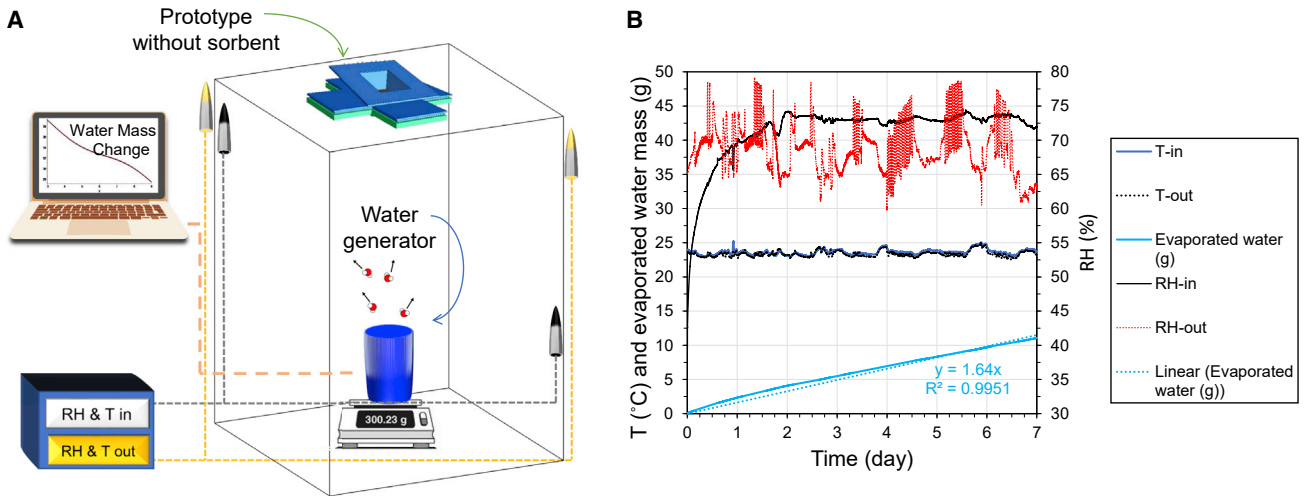

Figure 7. Scheme and sample results of the setup to test the humidity generation function using a 50-mL beaker (D = 4.8 cm) and containing 73 g water

(A) Scheme of the setup for testing. The box does not employ any sorbent.

(B) Indoor T and RH of the box. The test took place from March 16 to 24, 2022.

the humidity generator cannot reach its equilibrium RH (100%), also the rate of water evaporation from the beaker inside the box does not tend to zero. Both of these indicate that the box can still exchange water with the outside through the prototype's hole, so the water generator at the initial point was to reach equilibrium, and after reaching a higher RH than the outdoor, part of the evaporated water is sent outside. Equation 1 can be used to calculate the mass transfer coefficient of the box:

$$J_{w,t} = k_d \times (d_{in,t} - d_{out,t}), \quad \text{(Equation 1)}$$

where $J_{w,t}$ shows the mass transfer rate of water from inside the box to outdoor (g/s) at a time (t), k_d is the mass transfer coefficient (kg/s), and d represents the absolute humidity of air (g/kg), which can be calculated by:

$$d = 0.622 \frac{RH \times p_s}{B - RH \times p_s}, \quad \text{(Equation 2)}$$

where p_s is the saturated water vapor pressure and B stands for atmospheric pressure.

Since there is no water consumer in the system, all evaporating water is transferred outside, then:

$$equal J_{w,t} = \frac{\Delta m_{w,e,t}}{\Delta t} \quad \text{(Equation 3)}$$

$$J_w = \sum J_{w,t} = \sum \frac{\Delta m_{w,e,t}}{\Delta t} = k_d \sum (d_{in,t} - d_{out,t}), \quad \text{(Equation 4)}$$

where $\Delta m_{w,e,t}$ is the amount of evaporated water at each Δt time step. Assuming k_d is a constant and the mass evaporation linear during these 7 days, the overall evaporated water $m_{w,e}$ during these 7 days can be calculated as:

$$m_{w,e} = \sum \Delta m_{w,e,t} = k_d \times \Delta t \times \sum (d_{in,t} - d_{out,t}). \quad \text{(Equation 5)}$$

$m_{w,e}$ is known, which is the difference between initial and final beaker weight, equals 11.04 g. We measured the RH of 1-min intervals ($\Delta t = 1\ min$), and the difference between inside and outside absolute humidity of the air, d, can be calculated over

time. The mass transfer coefficient of this system (k_d) can thus be calculated as 2.33×10^{-5} kg s^{-1}. This value has a 25.8% error in comparison with real data. Although this error is relatively large, the mass transfer coefficient can be used in the real HP-AWH system to roughly calculate how much water is lost or gained during the test through the unsealed points. It should be emphasized that in this section we could use a sealed box, but to be able to use this calculated coefficient in the next section, the box with prototype frames and without sorbent inside is used here.

In the next section, we examine the dehumidifying and water production performance of our proposed HP-AWH system with selected sorbent (PS-20%) and humidity generator inside (a 50-mL water beaker).

Box with proposed HP-AWH prototype

The performance of our proposed HP-AWH is investigated by installing the prototype using a PS-20% sample (approximately 12.89 g) in the box containing a filled water beaker (containing 73 g water and an internal dimeter of 4.8 cm). The PS-20% sample was chosen because of its excellent sorption, desorption, and wicking properties, as well as the fact that it was less brittle than PS-30%, and it did not leak during the experiments at high RH. Initially, the RH of the box was increased to a value higher than 90% with the help of a commercial humidifier. Then the humidifier was removed, the prototype was installed immediately, and the box got sealed (see Note S10 and Figure S16 for more details). The indoor RH decreases over the first hours because of the presence of dry sorbent, and then gradually increases because the sorbent gets wet and loses its sorption capability, while water in the beaker is still evaporating into the box. The regeneration phase starts before reaching the maximum acceptable RH (with a 10% RH margin), and the center of the sample in the prototype is heated by an electric heater. The evaporated water from the desorption chamber during this phase is condensed on the silica wafer plate and collected in the designed vessel.

Although the idea of harvesting water from indoor humidity is exciting, it is crucial to emphasize that HP-AWH installation is first and foremost designed to dehumidify the interiors (not to harvest water), so we must continuously monitor and keep the indoor RH within the comfort zone. Comfort zones and limits can be determined using different approaches, such as ISO773, whose acceptable RH is defined between 30% and 70% according to the temperature range specified per season. Our test, with respect to this regulation, set the maximum acceptable RH limit at 70%, and activated the regeneration of sorbent also AWH function as soon as the RH reached 60% (to prevent passing of RH from the 70% during regeneration phase).

Figure 8 shows the mass of evaporated water, inside and out of the side RH and temperature of the box in 30 days. Even with a high evaporation rate from the water in the beaker, the RH dropped beneath 70% during the first 7 h of the test. In 17 h, the RH decreased below 60%, and this value was maintained for 80 h. According to the process described, the cyclic regenerating cycle was initiated when the indoor reached 60% (after almost 4 days), and the center of sorbent (located within the prototype's desorption chamber) was heated to 85 °C during each regeneration cycle by a 12-V electric heater. After 54 consecutive cycles with different RH levels, the results show that the proposed HP-AWH system maintains the RH in a comfortable range (between 50% and 68%), dampening the severe fluctuations in the RH (both at higher and lower outside RHs). More important, we could collect between 0.454 and 1.311 g of water per cycle. Table S6 shows the details for the of the experiments. There were collected 3.250 g, 1.897 g, 2.273 g, and 1.791 g of water in first

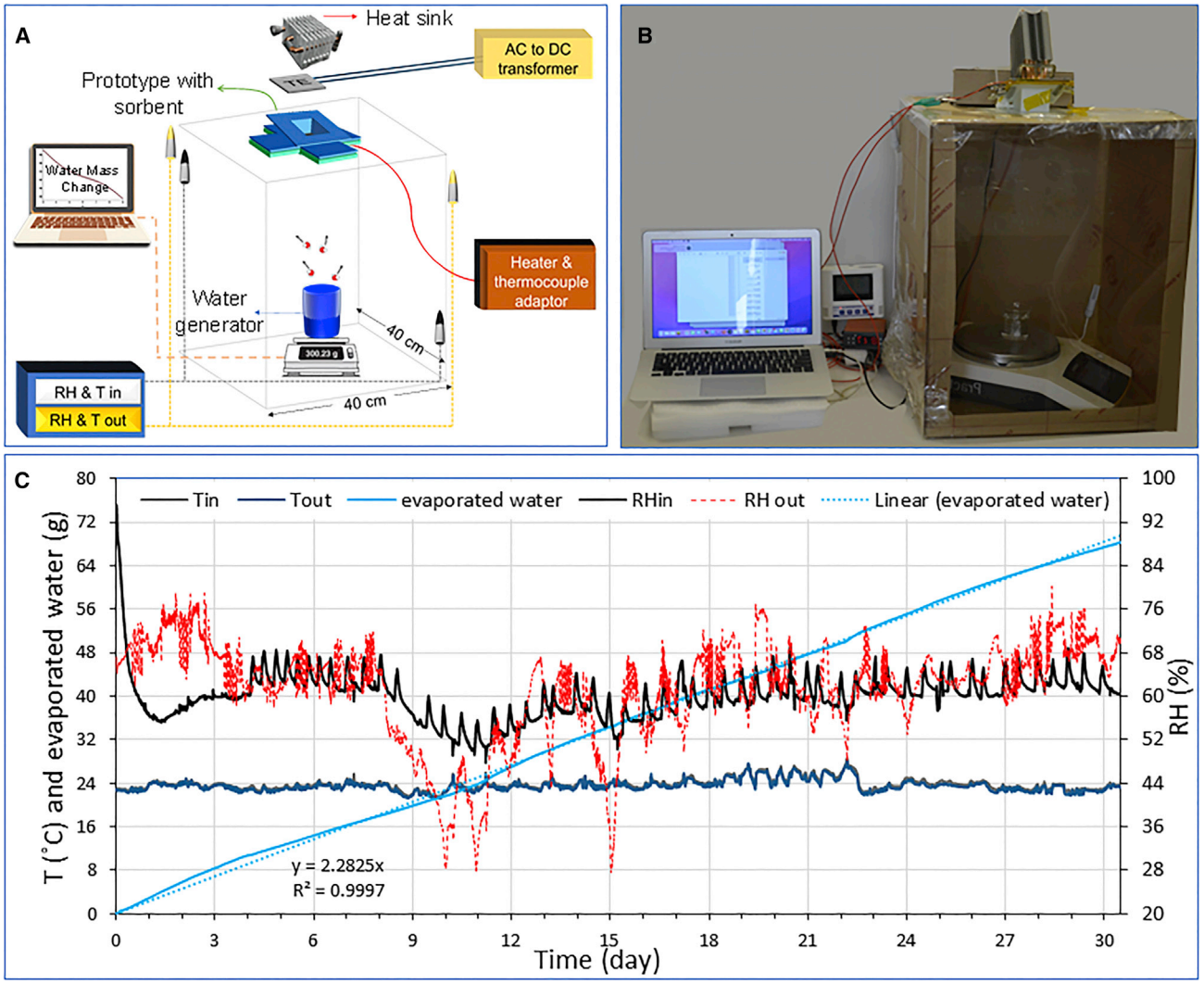

Figure 8. Scheme and real photo of the experiment setup for HP-AWH and its results

(A and B) Schematic (A) and an actual photo (B) of the HP-AWH in operation.

(C) Evaluation of HP-AWH performance over the course of one month by regulating the RH using 73 g water in a 50-mL beaker (D = 4.8 cm) as a humidity generator. Starting March 24, 2022.

day, second day, third day, and the fourth day, respectively (keep in mind that cycles intervals and regeneration time may differ in 1 day).

Water evaporation rate in this section of the experiments was approximately 2.28 g/d (equivalent to water generation from 3.3 people). The specific dehumidification rate is calculated as[12]:

$$r = \frac{\Delta m_t}{t.S} \quad \text{(Equation 6)}$$

$$\Delta m_t = \Delta m_{w,e,t} + \Delta m_d \quad \text{(Equation 7)}$$

Using this equation, Δm_t (g) represents the total amount of water (from humidity generator $\Delta m_{w,e,t}$ and dehumidification Δm_d) that is sent out of the model house at a known time (t), and S represents the total area of the sorbent in the frame (m^2). The total area of sorbent in this study is 124 cm^2 (excluding 0.5-cm margins

from each edge, which are not participating in sorption or desorption). Δm_d can be calculated as:

$$\Delta m_d = V\left(d_2\rho_{g2} - d_1\rho_{g1}\right), \quad \text{(Equation 8)}$$

where V is the volume of the model house (m^3) and ρ_g is the density of humid air (kg m^{-3}) at the working temperature and RH. Subscript 1 represents the point at which t began, and subscript 2 represents the point at which it ended. For example, in the first hour, the indoor RH decreased from 95.10% to 88.75%, and the water content correspondingly varied from 19.27 to 18.24 g kg^{-1}, resulting in Δm_d = 0.097g water dehumidification from the box. Considering the evaporation from the beaker, in the first hour of operation $\Delta m_{w,e}$ = 0.15 g water injected inside the box. This information leads to an average dehumidification rate of r = 19.94 g $m^{-2}\,h^{-1}$ at the first hour.

It should be noted that, during the seasons with lower temperatures, the RH is naturally low, and dehumidification is not necessary. So, we tested the device only at high temperatures. To prove the HP-AWH concept at higher temperatures, we repeated this test at temperature as high as 30 °C. The result shows that temperature does not affect the performance that much (see Note S11). Furthermore, in this study, we used composite prepared with a 20% salt solution to avoid potential leakage. Using PS-30% could have a higher moisture removal capacity but a higher risk of leakage. In terms of the condition that the risk of leakage is high, a breathable superhydrophobic membrane can be wrapped around the ACF composite to avoid leakage.[14,29] More optimization suggestions are provided in Note S12.

Water balance in HP-AWH

Using our proof-of-concept HP-AWH device, including the time-varying RH during the experiment as an input, we calculated the exchanged humidity between the model house and outdoors of each time step. Based on our results in the subsection on "Box with only humidity generation and without sorbent," the beaker inside the box tries to increase the RH to equilibrium (approximately 100%) while the sorbent sorbs this moisture and attempts to dehumidify the system. Also, the middle part of the sorbent is repeatedly heated to harvest a portion of the water captured by the sorbent wings, dehumidifying the box. Based on the water mass balance in the proposed HP-AWH system at steady state mode, there are two sources of water inputs: evaporation from the beaker and diffusion from the outside of the absolute humidity outside is higher. Water output includes water collected after performing AWH functions, and water that is diffused to the outdoors through the walls when the indoors is more humid. The fluctuation of the outside RH, coupled with the difficulty of maintaining the RH in a pre-defined range, makes it problematic to determine the exact amount of water that is exchanged between the box and the outdoors. Based on the average mass coefficient calculated in Equation 6, $k_d = 2.33\times10^{-5}$ kg s^{-1}, it is revealed that almost 1.81 g water is transferred inside the box (see Figure S15D), while 67.46 g water is injected into the box via a humidity generator, and 42.22 g of water is collected within the 30 days (approximately 61% of waste water), resulting in storing 27.05 g of water in the ACF body. We show good agreement between our experiments and model, and the final mass of stored water differs by less than 0.62 g. The discrepancy can be attributed to more water input from the prototype and walls of the box by diffusion from the prototype or side walls hole.

It is difficult to draw a direct comparison between our concept and previously reported experiments for several reasons. First, our experiments were performed for a whole month with vigorous humidity generation inside and different outdoor RH conditions, while previously reported studies only lasted for a maximum of 2 h

and without any humidity generator inside. In addition, our concept has only 4 h of regeneration time per day, while other systems need continuous 24 h regeneration to maintain RH in a comfortable range. Also, some studies used sunlight for regeneration; however, their systems cannot operate during the nights, which is two times longer than daytime.[12,13] Additionally, the size of the testing box, material, and total mass of adsorbent varied in different studies. More important, our study is the first study that could experimentally couple one of the newly developed desiccant-based dehumidification systems with AWH, so there is no similar work for comparison.

Scaling up

To describe a scale-up HP-AWH and evaluate this concept in a real building, we need to know the various parameters needed to design the system to deal with latent heat. In view of previous studies, the sorbent was used in a small box (80,000 cm^3) that has 88 cm^2 of sorbent surface (30 cm^2 of the margins are below the lower body and are not included in sorption) and 36 cm^2 of desorption surface. Our findings indicate that the ratio of sorption to desorption sites (approximately 88:30) is acceptable, and the wicking performance allows water to pass through all sorbents effectively. To scale up the HP-AWH system, the sorbent surface-to-interior volume ratio needs to be kept constant (124 cm^2: 0.08 m^3). Based on our experimentation, we estimate that we will need 12.4 m^2 of sorbent to dehumidify a real room 80 m^3 in size (accommodating three people). With this amount of sorbent, the RH could be decreased from near saturated to less than 70% without causing any temperature increase while maintaining this temperature for a long time. Better still, this dehumidification can result in a 1 $^\circ C$ decrease in the heat index and produce 1.3–3.2 kg water per day from residents' exhaled moisture. It should be noted that ACF wicks water up to a height of 10 cm, so it is best applied to horizontal configurations for bungalows rather than vertical configurations for apartment exterior walls. In apartments, a tank of LiCl can be installed at the top of each floor to provide gravity-driven water wicking down.

Energy consumption, moisture removal capacity, and cost

The ASHRAE 90.1 standard specifies that dehumidification equipment must have a minimum efficiency of 1.8 kg/kWh. For the entire 30-day process, the moisture removal efficiency of the HP-AWH prototype is 0.18 kg/kWh, which can be significantly improved. It is important to stress that this is a prototype to prove that the HP-AWH concept is practical and that we designed these experiments in accordance with the time schedule of students who were conducting the test. Consequently, we have not tried to maximize the efficiency of this system. First, our random checks of a few cycles revealed that, in all tested cycles, more than 70% of the total amount of water produced was collected within the first hour. Accordingly, three 1-h cycles every 8 h could produce the same amount of water as two 2-h cycles (every 12 h) and consume 25% less energy than two 2-h cycles. Second, we considered the ratio of sorption surface to desorption sites surface (88:30). This was dictated by the fact that, to prove our concept, we had to have at least one desorption site positioned between sorption sites (to ensure that the desorption site does not have a dead zone). In subsequent studies, the ratio could be increased to 50:50, in which there would be no dead zones in the sorption sites as well, thereby reducing the desorption time and crystallization risk. Concerning crystallization, it would be a great opportunity for sorbents that do not contain salt and rather use hydrogels.[4,30–32] or nanoparticles such as MOF[24,33] and Ppy-Cl[34] for water sorption.

Furthermore, the sorbent in our system has not been fully regenerated in our attempt to avoid crystallization. The heat storage capacity of ACF-LiCl-based

composites is over 1.5 kWh kg^{-1},[17] so heating it is energy consuming as it holds a great amount of heat, which is wasted during cooling processes two or three times daily (while AWH is a mono cycle and wastes this heat once a day). By using non-salt sorbents, the desorption site can be fully regenerated and produce at least five times more water than it does currently (27 g water is stored in the PS sample, which is at least 20% of the total amount of water). Also, a higher water input will increase the efficiency of the system. As an example, in the first cycle, the moisture removal efficiency is 0.37 kg/kWh, which is twice the average value. Thus, the system performs very well under real-world conditions, where an air change of 0.5 per hour is recommended for the provision of sufficient fresh air in residential spaces.

In addition, this system has a very low capital cost (see Note S13) and does not produce any greenhouse gas emissions in terms of embodied energy or refrigerants (these two components comprise 41% of greenhouse gas emissions from air conditioning in 2016[2]). As a result of these factors, it can be concluded that the system will be able to meet the energy requirements, however, with the current information, it is not possible to calculate the exact efficiency, which leaves a research gap for future studies. There will likely be a need for multidisciplinary research teams, which will include experts in thermal sciences and mechanical engineering in addition to experts in separation technologies, materials science, and chemistry.

Finally, it is worth mentioning that IR-emitters technology is no longer limited to the nighttime, and recent findings show 3 °C –15 °C sub-ambient cooling performance, 63–72.7 W m^{-2} cooling power under direct sunlight, and a cooling performance of 9 °C at night.[20,21,35] Therefore, it seems reasonable to use IR-cooling emitters in the condenser of our proposed system. However, since their power density is low, and the condenser is critical during the regeneration period, phase change material can be used for cold storage around the clock for desorption half-cycles.

DISCUSSION

Climate change has caused an increased the need to cool the air in our built environment. Globally, air conditioning contributes 3.9% to greenhouse gas emissions. In comparison with decreasing the air temperature (i.e., cooling air), decreasing the air humidity (i.e., removing water vapor from the air) produces more emissions. These emissions are expected to increase dramatically with the increase in cooling demand around the world. This has led to an increased interest in humidity control in buildings. In addition to reducing the humidity in the buildings, the extracted humidity from a building's interior can be a potential source of water.

Based on the adaptation of the intrinsic water pump system of trees, which absorbs water from the roots and releases it to the leaves to transpire and create continuous pumping of water (nutrition), we propose an HP system that uses sorbents with capillary effect to capture water molecules within the sorption site located indoor (roots) and transfer them to the outdoors (leaves) to evaporate. This creates a continuous driving force for natural water flow with several advantages, which include (1) replacing the moving parts of dehumidifiers such as HP with passive water wicking force, (2) decreasing energy consumption for regeneration by effectively shortening the regeneration cycles to two to three times per day in a smaller surface area, and (3) increasing the potential of collecting extracted water from indoor due to discontinuous but high concentration water vapor resource during regeneration. Additionally, this proposed HP-AWH system presents a compact design as it is simply installed on the roof of a building.

We tested this concept using traditional activated carbon felts (ACFs) composites that are commercially available and have a high moisture absorbing capability, as well as high capillary to transfer the absorbed water from a surface exposed to the humid air to the insulated parts. The capillary effect of ACF, which transfers water from the sorption to the desorption sites, is an important characteristic that has been overlooked over the years. Our results indicate that, if one-half of the surface of ACF-LiCl composites is exposed to high-humidity air, more than 50% of the absorbed water will be stored in the other covered one-half. We thereafter developed a prototype of the HP-AWH system consisting of a condenser and two frames that hold a sorbent with four wings exposed to the indoor for sorption and connected at the center. Our prototype was installed in a 1,000 times down-scale room and our 30-day tests indicate that it can produce 1.3–3.25 g of water per day while maintaining an RH between 50% and 70% with no sensible increase in the temperature inside. Unlike previous studies, our tests were not conducted with a sealed box, but with a water container from which water vapor was continuously withdrawn to increase humidity to the saturation condition (RH = 100%). Even with high fluctuations in the humidity outside, the indoor humidity was regulated, and liquid water was produced in each regeneration cycle (approximately 61% of extracted water was recycled). Our system shows a 2,600% energy improvement compared to previous studies which used thermoelectric. We also used an IR cooling emitter, which can serve as a cold surface to act as a condenser for the AWH system. To the best of our knowledge, there has not been any previous study on the HP-AWH system, and this continuous indoor dehumidification in the presence of a humidity generator with periodic water production using daytime cooling is an entirely new concept. This work reveals that an ACF-based desiccant and IR-cooling can be potentially applied in sustainable buildings for simultaneous dehumidification and efficient AWH.

EXPERIMENTAL PROCEDURES

Resource availability

Lead contact

Further information and requests for resources and materials should be directed to and will be fulfilled by the Lead Contact, Liang An (liang.an@polyu.edu.hk) or Ruzhu Wang (rzwang@sjtu.edu.cn).

Materials availability

This study did not generate unique materials.

Data and code availability

Details about the experiments, model equations and their implementation and the data used to conclude can be found in the article and the Supporting Information. Raw data from Figures 4, 5, 6, 7, 8, S11, S12, S15, S16, and S17 were deposited on Mendeley at https://doi.org/10.17632/fn5624tpx5.1. Requests for further information should be directed to the lead contact.

Materials and fabrication of the sorbent layers

Materials

Lithium chloride (98%) was purchased from Aladdin. ACF was purchased from Long Shengbao, China. Deionized water (18.2 MU) was used throughout the experiment.

IR-cooling sample

As part of the fabrication of the IR-cooling emitter, Ag and Cr are deposited on a JGS2 fused silica wafer using plasma-based physical vapor deposition (Denton Explorer 14 Sputtering System). The parameters are mentioned in S5. PDMS Sylgard 184 from Dow Corning was spin-coated on the same side of the wafer in a 10:1

mix of prepolymer: curing agent. The parameters were 580 rpm, 60 s duration, and 20 rps acceleration. The samples were then cured for 1 h at 80°C after spin coating.

Square samples

Four pieces of ACF were cut into 5 cm × 5 cm squares, and immersed in LiCl solutions of 5%, 10%, 20%, and 30% (wt %) vertically for 24 h. Afterward, the samples were dried at 80°C for 24 h. They were labeled "5%-Square," "10%-Square," "20%-Square," and "30%-Square," respectively.

Another piece of ACF is cut to 5 cm × 5 cm and placed between nonwoven cotton paper, and immersed in 30% LiCl solution for 24 h. The samples are then dried for 24 h at 80 °C. It was labeled "30%-Square-Wrap."

Wick samples

Four pieces of 5 cm × 10 cm dry ACF were cut, hung in LiCl solutions of 5%, 10%, 20%, and 30% (wt %) vertically for 12 h and then flipped from the other end and left in the solution for another 12 h. We left both ends of the samples in the salt solution at the last hour. The samples were removed and dried at 80 °C for 24 h. Accordingly, they were labeled "5%-wick," "10%-wick," "20%-wick," "30%-wick," and so forth.

An additional 5 cm × 10 cm piece of dry ACF was wrapped in nonwoven cotton paper, and immersed in a 30% LiCl solution for 24 h. After the sample was taken out, it was dried at 80 °C for 24 h. The sample labeled as "30%-Wick-Wrap."

Prototype samples

A (+) shape was created for the samples used in the prototype. By using this shape, it is less likely that solid LiCl crystals remain unsolved in the sorbent, and it is easier to install compared to a circle shape. Figure S7 illustrates the exact dimensions of this shape. Initially, ACF is cut into this shape and immersed in a 20% or 30% solution. After immersing the samples in a salt solution for 24 h, the samples were taken out of the solution and placed on a glass plate. To adjust the edge of samples before drying, we use a pattern underneath a glass plate since the ACF shape changes during immersion, and the composite material is fragile once dry. The composite is then dried at 60 °C. After 3 h of heating, the sorbent was flipped to prevent it from sticking to the plate and then it was heated at 80 °C for another 24 h. The samples were labeled prototype sample (PS)-20% and PS-30%, where the numbers refer to the concentration of the used salt solution.

Absorption tests

Samples were placed in a constant humidity and temperature chamber for a duration of 10 h at a temperature of 30 °C and an air RH of 40% or 70%. Using 0.001 g accuracy electronic balance scales, we weighed and recorded samples based on a schedule table.

Since all ACF samples originate from the same ACF, they have a thickness of approximately 2 mm. It is, however, difficult to determine the exact thickness. Therefore, in this study, we determined the volumetric sorption capacity of each sample by measuring the amount of sorbed water on the surface area (× surface [kg m^{-2}]).

Fabrication of prototypes

According to the earlier design optimization, the prototype HP-AWH was built. This device consists of a lower part (Nylon PA12) and an upper part (resin) that were fabricated using 3D printing technology. These frames will assemble to hold a "+" shape

sorbent, a condenser, and a heater with its insulation. The detail of this prototype is reported in Note S5.

SUPPLEMENTAL INFORMATION

Supplemental information can be found online at https://doi.org/10.1016/j.xcrp.2023.101278.

ACKNOWLEDGMENTS

Fully supported by a grant from the National Natural Science Foundation of China (No. 52022003). In this research work, we acknowledge the assistance provided by the University Research Facility in 3D Printing.

AUTHOR CONTRIBUTIONS

A.E. conceptualized the work and characterized the ACF-LiCl material properties. A.E. designed the prototype and experimental setup. A.E. fabricated the prototype, sorbent, and IR-emitter experimental setup, and conducted the experiments. A.E. performed optical characterization, and water quality measurements. A.E., L.H., and O.C.E. wrote the initial paper with input from all other authors. W.L. performed isotherms and pore characterization tests. R.Y. provided facilities for testing. L.A. and R.Z.W. participated in writing and editing the final manuscript. L.A., R.Y., and R.Z.W. guided the project and supervised the work.

DECLARATION OF INTERESTS

The authors declare no competing interests.

Received: August 20, 2022
Revised: December 6, 2022
Accepted: January 12, 2023
Published: January 30, 2023

REFERENCES

1. Fact Sheet, HVAC Energy Breakdown, Department of the Environment and Energy, https://www.energy.gov.au/sites/default/files/hvac-factsheet-energy-breakdown.pdf, Retrieved on : 11.24.2021.

2. Woods, J., James, N., Kozubal, E., Bonnema, E., Brief, K., Voeller, L., and Rivest, J. (2022). Humidity's impact on greenhouse gas emissions from air conditioning. Joule *6*, 726–741. https://doi.org/10.1016/j.joule.2022.02.013.

3. Haechler, I., Park, H., Schnoering, G., Gulich, T., Rohner, M., Tripathy, A., Milionis, A., Schutzius, T.M., and Poulikakos, D. (2021). Exploiting radiative cooling for uninterrupted 24-hour water harvesting from the atmosphere. Sci. Adv. *7*, eabf3978. https://doi.org/10.1126/sciadv.abf3978.

4. Dai, M., Zhao, F., Fan, J., Li, Q., Yang, Y., Fan, Z., Ling, S., Yu, H., Liu, S., Li, J., et al. (2022). A nanostructured moisture-absorbing gel for fast and large-scale passive dehumidification. Adv. Mater. 2200865. https://doi.org/10.1002/adma.202200865.

5. Zhang, X., Yang, J., Qu, H., Yu, Z.G., Nandakumar, D.K., Zhang, Y., and Tan, S.C. (2021). Machine-learning-assisted autonomous humidity management system based on solar-regenerated super hygroscopic complex. Adv. Sci. *8*, 2003939. https://doi.org/10.1002/advs.202003939.

6. Zheng, X., Ge, T.S., and Wang, R.Z. (2014). Recent progress on desiccant materials for solid desiccant cooling systems. Energy *74*, 280–294. https://doi.org/10.1016/j.energy.2014.07.027.

7. Ma, Q., and Zheng, X. (2022). Preparation and characterization of thermo-responsive composite for adsorption-based dehumidification and water harvesting. Chem. Eng. J. *429*, 132498. https://doi.org/10.1016/j.cej.2021.132498.

8. Audah, N., Ghaddar, N., and Ghali, K. (2011). Optimized solar-powered liquid desiccant system to supply building fresh water and cooling needs. Appl. Energy *88*, 3726–3736. https://doi.org/10.1016/j.apenergy.2011.04.028.

9. Duong, H.C., Hai, F.I., Al-Jubainawi, A., Ma, Z., He, T., and Nghiem, L.D. (2017). Liquid desiccant lithium chloride regeneration by membrane distillation for air conditioning. Separ. Purif. Technol. *177*, 121–128. https://doi.org/10.1016/j.seppur.2016.12.031.

10. Gido, B., Friedler, E., and Broday, D.M. (2016). Liquid-desiccant vapor separation reduces the energy requirements of atmospheric moisture harvesting. Environ. Sci. Technol. *50*, 8362–8367. https://doi.org/10.1021/acs.est.6b01280.

11. Li, B., Hua, L., Tu, Y., and Wang, R. (2019). A full-solid-state humidity pump for localized humidity control. Joule *3*, 1427–1436. https://doi.org/10.1016/j.joule.2019.03.018.

12. Cao, B., Tu, Y., and Wang, R. (2019). A moisture-penetrating humidity pump directly powered by one-sun illumination. iScience *15*, 502–513. https://doi.org/10.1016/j.isci.2019.05.013.

13. Zhang, Y., Wu, L., Wang, X., Yu, J., and Ding, B. (2020). Super hygroscopic nanofibrous membrane-based moisture pump for solar-driven indoor dehumidification. Nat. Commun. *11*, 3302. https://doi.org/10.1038/s41467-020-17118-3.

14. Shan, H., Pan, Q., Xiang, C., Poredoš, P., Ma, Q., Ye, Z., Hou, G., and Wang, R. (2021). High-yield solar-driven atmospheric water harvesting with ultra-high salt content composites encapsulated in porous membrane. Cell Rep. Phys. Sci. *2*, 100664. https://doi.org/10.1016/j.xcrp.2021.100664.

15. Entezari, A., Ejeian, M., and Wang, R.Z. (2019). Extraordinary air water harvesting performance with three phase sorption. Mater. Today Energy *13*, 362–373. https://doi.org/10.1016/j.mtener.2019.07.001.

16. Ejeian, M., Entezari, A., and Wang, R.Z. (2020). Solar powered atmospheric water harvesting with enhanced LiCl/MgSO4/ACF composite. Appl. Therm. Eng. *176*, 115396. https://doi.org/10.1016/j.applthermaleng.2020.115396.

17. Liu, X.Y., Wang, W.W., Xie, S.T., and Pan, Q.W. (2021). Performance characterization and application of composite adsorbent LiCl@ACFF for moisture harvesting. Sci. Rep. *11*, 14412. https://doi.org/10.1038/s41598-021-93784-7.

18. Wang, J.Y., Wang, R.Z., Tu, Y.D., and Wang, L.W. (2018). Universal scalable sorption-based atmosphere water harvesting. Energy *165*, 387–395. https://doi.org/10.1016/j.energy.2018.09.106.

19. Wang, J.Y., Wang, R.Z., and Wang, L.W. (2016). Water vapor sorption performance of ACF-CaCl2 and silica gel-CaCl2 composite adsorbents. Appl. Therm. Eng. *100*, 893–901. https://doi.org/10.1016/j.applthermaleng.2016.02.100.

20. Zhu, Y., Ye, Y., Wang, D., and Cao, Y. (2021). Simple dual-layer emitter for daytime radiative cooling. OSA Continuum *4*, 416–427. https://doi.org/10.1364/OSAC.398685.

21. Zhou, L., Rada, J., Zhang, H., Song, H., Mirniaharikandi, S., Ooi, B.S., and Gan, Q. (2021). Sustainable and inexpensive Polydimethylsiloxane sponges for daytime radiative cooling. Adv. Sci. *8*, 2102502. https://doi.org/10.1002/advs.202102502.

22. Zheng, X., Ge, T.S., Wang, R.Z., and Hu, L.M. (2014). Performance study of composite silica gels with different pore sizes and different impregnating hygroscopic salts. Chem. Eng. Sci. *120*, 1–9. https://doi.org/10.1016/j.ces.2014.08.047.

23. Zheng, X., Wang, R.Z., and Ge, T.S. (2016). Experimental study and performance predication of carbon based composite desiccants for desiccant coated heat exchangers. Int. J. Refrig. *72*, 124–131. https://doi.org/10.1016/j.ijrefrig.2016.03.013.

24. Kim, H., Yang, S., Rao, S.R., Narayanan, S., Kapustin, E.A., Furukawa, H., Umans, A.S., Yaghi, O.M., and Wang, E.N. (2017). Water harvesting from air with metal-organic frameworks powered by natural sunlight. Science *356*, 430–434. https://doi.org/10.1126/science.aam8743.

25. Tu, Y., Wang, R., Zhang, Y., and Wang, J. (2018). Progress and expectation of atmospheric water harvesting. Joule *2*, 1452–1475. https://doi.org/10.1016/j.joule.2018.07.015.

26. Zhang, S., Chi, M., Mo, J., Liu, T., Liu, Y., Fu, Q., Wang, J., Luo, B., Qin, Y., Wang, S., and Nie, S. (2022). Bioinspired asymmetric amphiphilic surface for triboelectric enhanced efficient water harvesting. Nat. Commun. *13*, 4168. https://doi.org/10.1038/s41467-022-31987-w.

27. Zheng, X., Ge, T.S., Hu, L.M., and Wang, R.Z. (2015). Development and characterization of mesoporous silicate–LiCl composite desiccants for solid desiccant cooling systems. Ind. Eng. Chem. Res. *54*, 2966–2973. https://doi.org/10.1021/ie504948j.

28. Entezari, A., Ge, T.S., and Wang, R.Z. (2018). Water adsorption on the coated aluminum sheets by composite materials (LiCl + LiBr)/silica gel. Energy *160*, 64–71. https://doi.org/10.1016/j.energy.2018.06.210.

29. Wang, Y., Gao, S., Zhong, H., Zhang, B., Cui, M., Jiang, M., Wang, S., and Wang, Z. (2022). Heterogeneous wettability and radiative cooling for efficient deliquescent sorbents-based atmospheric water harvesting. Cell Reports Physical Science *3*, 100879. https://doi.org/10.1016/j.xcrp.2022.100879.

30. Lu, H., Shi, W., Zhang, J.H., Chen, A.C., Guan, W., Lei, C., Greer, J.R., Boriskina, S.V., and Yu, G. (2022). Tailoring the desorption behavior of hygroscopic gels for atmospheric water harvesting in arid climates. Adv. Mater. *34*, 2205344. https://doi.org/10.1002/adma.202205344.

31. Guo, Y., Guan, W., Lei, C., Lu, H., Shi, W., and Yu, G. (2022). Scalable super hygroscopic polymer films for sustainable moisture harvesting in arid environments. Nat. Commun. *13*, 2761. https://doi.org/10.1038/s41467-022-30505-2.

32. Lu, H., Shi, W., Guo, Y., Guan, W., Lei, C., and Yu, G. (2022). Materials engineering for atmospheric water harvesting: progress and perspectives. Adv. Mater. *34*, 2110079. https://doi.org/10.1002/adma.202110079.

33. Yilmaz, G., Meng, F.L., Lu, W., Abed, J., Peh, C.K.N., Gao, M., Sargent, E.H., and Ho, G.W. (2020). Autonomous atmospheric water seeping MOF matrix. Sci. Adv. *6*, eabc8605. https://doi.org/10.1126/sciadv.abc8605.

34. Zhao, F., Zhou, X., Liu, Y., Shi, Y., Dai, Y., and Yu, G. (2019). Super moisture-absorbent gels for all-weather atmospheric water harvesting. Adv. Mater. *31*, 1806446. https://doi.org/10.1002/adma.201806446.

35. Li, P., Wang, A., Fan, J., Kang, Q., Jiang, P., Bao, H., and Huang, X. (2021). Thermo-optically designed scalable photonic films with high thermal conductivity for subambient and above-ambient radiative cooling. Adv. Funct. Mater. 2109542. https://doi.org/10.1002/adfm.202109542.